IEEE Access
Multidisciplinary | Rapid Review | Open Access Journal

Received April 16, 2021, accepted June 26, 2021, date of publication July 5, 2021, date of current version July 14, 2021.

Digital Object Identifier 10.1109/ACCESS.2021.3094892

A Molecular Communication-Based Simultaneous Targeted-Drug Delivery Scheme

TANIA ISLAM, (Graduate Student Member, IEEE), ETHUNGSHAN SHITIRI, (Member, IEEE), AND HO-SHIN CHO, (Senior Member, IEEE)
School of Electronic and Electrical Engineering, Kyungpook National University, Daegu 41556, South Korea

Corresponding author: Ho-Shin Cho (hscho@ee.knu.ac.kr)

This work was supported by the National Research Foundation of Korea (NRF) grant funded by the Korea Government [Ministry of Science, ICT and Future Planning (MSIT)] 2021R1A2C1003507.

ABSTRACT This paper considers simultaneous drug-delivery (SDD) in molecular communication-based (MC-based) targeted drug-delivery systems. In a realistic scenario, the drug-carrying nanomachines are randomly placed close to the infected site. Due to the random propagation delays in the MC channel, the drugs from multiple drug-carrying nanomachines may, therefore, not arrive simultaneously at the infected site, leading to low efficacy and resulting in drug-delivery-time errors. To overcome this error and to administer the drugs simultaneously at the infected site, we use an internal controller nanomachine to control the release times of the drug-carrying nanomachines, with consideration of the propagation delay, to achieve SDD. In this regard, we propose two SDD schemes, namely, the direct trigger estimate SDD (DTE-SDD) scheme and the indirect trigger estimate SDD (iDTE-SDD) scheme. The difference between these schemes is that in the iDTE-SDD scheme, to estimate the propagation delay, the internal controller nanomachine depends on the drug-carrying nanomachines, while in the DTE-SDD scheme, it does not. Furthermore, to study the errors theoretically, we derive the analytical model of delivery-time error, and this is validated with simulation results. We perform intensive evaluations to understand the system's behavior under different channel conditions, such as the number of molecules released and the distance. The simulation results highlight the proposed scheme's energy efficiency and robustness to the large propagation delay, reducing the delivery-time error to improve the accuracy of the SDD.

INDEX TERMS Molecular communication, nanonetworks, nanomedicine, targeted drug delivery.

I. INTRODUCTION

Molecular communication (MC) is a bio-inspired communication paradigm that facilitates the understanding and modeling of communication between the biological nanomachines in aqueous micro-environments on nano-to-micro scales [1], [2]. In MC via diffusion (MCvD), information between the bio-nanomachines (e.g., living cells) is exchanged through the free diffusion of molecules that propagate randomly via Brownian motion in fluidic biological micro-environments (e.g., blood vessels, biological tissues) [3]–[5]. Due to its biocompatibility and lower energy requirements, MCvD is ideally suited for biomedical applications, such as targeted drug delivery (TDD), the monitoring of health conditions, lab-on-a-chip systems, inter-cellular communication via neuro-transmitters, and inter-organ communication [6]–[8].

Among the applications, TDD is one of the most promising [9], [10]. It is a drug-delivery system that is designed to perform localized administration of drugs to the target or infected site; thus, it can prevent the drug from spreading to the surrounding healthy areas of the body [9], [11]. To avert damage to healthy areas, as well as drug degradation, the drug molecules are encapsulated in the nanomachines [12]. Typically, nanomachines are on a nano-to-micro meter scale; therefore, they can be deployed directly to the infected site of the body (local drug-delivery system), or they can be inserted through the cardiovascular system (systemic drug-delivery system) [12]–[16]. Once the nanomachines are in the desired positions, they can release the drugs in response to internal trigger stimuli (e.g., the environmental pH or the

The associate editor coordinating the review of this manuscript and approving it for publication was Liangtian Wan.

temperature) or external trigger stimuli (e.g., ultrasound or magnetic triggering) [17]–[19]. The TDD system that uses MC as the communication paradigm will be referred to as the *molecular communication-based targeted drug-delivery* (MC-based TDD) system.

In MC-based TDD, the nanomachine is the basic functional unit that can perform very simple and specific tasks (e.g., basic computing, data storage, actuation, or sensing) due to its short-range communication, limited energy, and low computational power [1], [20]. Additionally, nanomachines are limited in reservoir capacity. Therefore, to maintain the efficacy (maximum achievable therapeutic response from an administered drug) at the infected site, multiple coordinated nanomachines are required to share the burden of releasing the total amount of the drug. For example, a 10 mol/m^3 drug molar concentration, equivalent to 6.022×10^{18} molecules/cm^3, has been shown to produce substantial apoptosis for a circular tumor of radius 2.5 *cm* [21], [22]. Therefore, each nanomachine can release a small fraction of the drug, and the drug's cumulative concentration that would be sufficient to produce apoptosis is expected at the infected site. It is possible to administer single or multiple types of drugs using an MC-based TDD system [9], [23]. The former is called a single-drug-delivery system, while the latter one is called a multi-drug-delivery system. In this paper, we focus on a single-drug-delivery system.

Regardless of the number of the types of drug being administered, the drug concentration at the infected site needs to be within a specific therapeutic index (TI) to preserve efficacy. The TI is the range of drug concentrations at which a drug is effective [24]. The maximum safe concentration (MSC) and the least effective concentration (LEC) are the TI's upper and lower bound, respectively. The MSC is the utmost concentration level above which toxic effects of the drugs occur, and the LEC is the minimum drug concentration level at which the drug's efficacy is achieved [25]. Therefore, to efficiently obtain the cumulative concentrations of drugs to reach the LEC, the delivery of drug molecules from multiple nanomachines at the infected site must be at the same time, leading to *simultaneous drug delivery* (SDD). The challenge is that the nanomachines are at random distances from the infected site, which could lead to nonsimultaneous delivery. Consequently, the drug concentration may not exceed the LEC. Thus, it is necessary to coordinate the nanomachines' release times to ensure a simultaneous drug arrival time while reducing the complexity of the MC-based TDD system. For the remainder of this paper, the term *release time* is used to refer to the release time of the drugs from the drug-carrying nanomachines and the term *delivery time* is used to denote the arrival time of the drugs at the infected site.

Different researchers have proposed a variety of MC-based TDD systems. The transmission control protocol (TCP) like communication protocol was investigated in [15], where a three-dimensional (3D) communication channel is considered with static nanomachines, such as the local TDD system. Their work was developed to control the suitable release rate between transmitter and receiver nanomachines and to mitigate drug congestion at the receiver nanomachine. Analogously, to minimize the congestion at the infected site, in [14], the authors considered the relationship between the release rate and the number of receptors at the nanomachines. Similarly, in [26], an early congestion detection and release rate control protocol has been proposed in which one nanomachine acts as a controller, and the other one acts as an actuator that releases the drug molecules based on the command from the controller. A release rate control mechanism has been proposed in [22] that considers the distances of the nanomachines from the infected site. However, maintaining the release rate may not ensure the preservation of SDD when the nanomachines are at different distances from the destination. Therefore, suitable release times can ensure SDD when the nanomachines are at random distances from the infected site.

To achieve coordination among the drug-carrying nanomachines to realize SDD, synchronization schemes using timestamps [27], [28] could be implemented. For example, the release time can be encoded in the message after the completion of the synchronization phase. However, if an attempt were made to expand the coordination scheme in [27], [28] to achieve SDD, then the schemes in [27], [28] would require a large signaling overhead, a complex estimator (maximum likelihood estimation) to estimate the perturbation issues [29] (e.g., clock skew and clock offset), and an increased energy cost [27], [28]. Furthermore, the above-mentioned MC-based TDD systems are not tailored to address the SDD problem for nanomachines at random distances. For the first time in the MC-based TDD literature, the author in [23] introduced the SDD of equidistant nanomachines. Therefore, this paper aims to investigate the SDD for random distant nanomachines, where a simultaneous release cannot guarantee an SDD due to the propagation delay that varies with the distance [30]. This leads to the *delivery-time error* when the drug molecules from multiple nanomachines, which are expected to arrive at the infected site simultaneously, do not arrive simultaneously. The delivery-time error is the difference between the maximum and the minimum delivery times. We note that reducing the delivery-time error may improve the efficacy of the TDD system. From a communication engineer's point of view, this study focuses solely on the communication protocol to reduce the delivery-time error.

Therefore, considering the nanomachine's limited capacity, as well as being inspired by the observed benefits of not using timestamps relating to energy and complexity [29], in this paper, we investigate the communication protocol for SDD. We consider a 3D diffusive environment without drift in the channel [28], [29]. Unlike the work in [23], where the drug-carrying nanomachines were equidistant from the target, in this paper, different distances for the drug-carrying nanomachines are adopted. To the best of our knowledge, this is the first investigation of SDD for random distances. The main contributions of this paper are as follows:

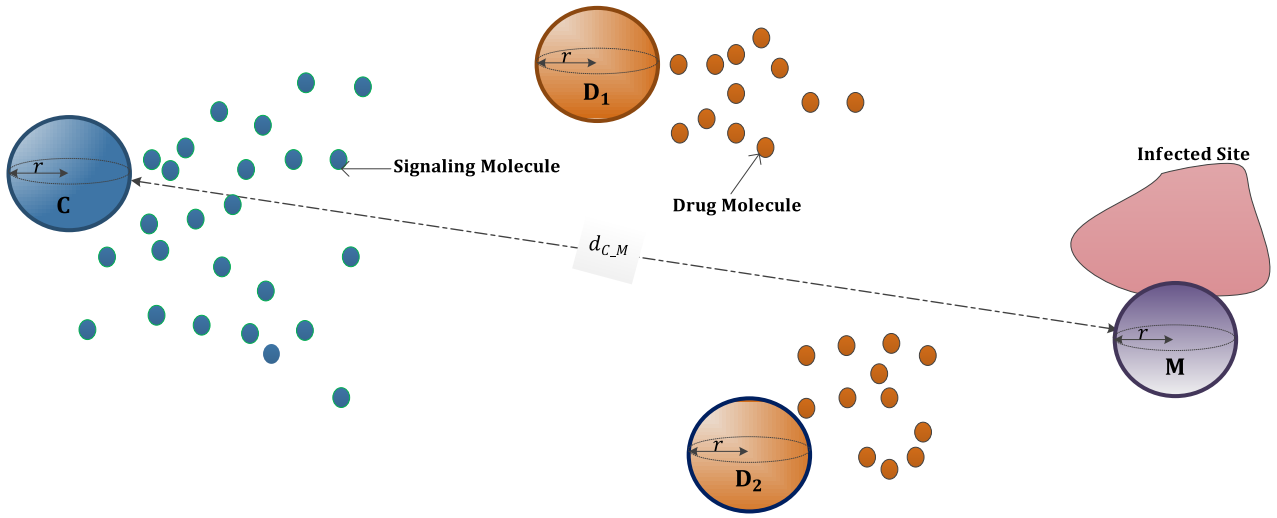

FIGURE 1. System model of an MC-based TDD system. C, D_1, D_2, and M denote the control nanomachine, drug-carrying nanomachine 1, drug-carrying nanomachine 2, and monitoring nanomachine, respectively.

- We define the drug-delivery-time error in MC-based TDD systems. By considering different propagation delay estimation approaches, we propose two novel internal controller-based energy-efficient SDD systems to reduce the delivery-time error, namely, the direct trigger estimate SDD (DTE-SDD) scheme and the indirect trigger estimate SDD (iDTE-SDD) scheme.
- We analyze the impact of the number of released molecules and the distances of the nanomachines on the SDD time.
- We also investigate the energy consumption of the proposed schemes by varying the number of drug-carrying nanomachines.
- Finally, we develop an analytical model for simultaneous drug-delivery-time error and validate it using computer simulation. Furthermore, to illustrate the gains of the proposed schemes in terms of energy expenditure and error, we compare the proposed schemes with a timestamp scheme.

The remainder of this paper is organized as follows. Section II represents the system model. In Section III, description of the operation of the proposed schemes is provided. Numerical analysis is presented in Section IV. Finally, we conclude this paper with proposals for future directions in Section V. Unless otherwise stated, Table 1 describes the notations used in this paper.

TABLE 1. Notations used to explain the proposed schemes.

Symbol	Description
C	control nanomachine
D	drug-carrying nanomachine
M	monitoring nanomachine
Q	number of emitted molecules
N	number of Ds
d_{x_y}	distance between x and y where x,$y \in \{C, D_i, M\}$ and $i \in N$
Ω	diffusion coefficient
INI	initiation signal
RES	response signal
RLY	relay signal
EMS	estimation signal
ERS	estimation response signal
DRR	drug-releasing signal
τ_{x_y}	propagation delay between x and y
$\tau_{x\_y}^{(z)}$	propagation delay between x and y where z denotes the signal sending event
T_Σ	common delivery-time
ε	delivery-time error

II. SYSTEM MODEL

We consider four static transceiver nanomachines in an unbounded 3D environment in which all the nanomachines are assumed to be spherical bodies with a radius, r, as shown in Fig. 1 [14], [22], [31]–[33]. We consider the transmitting nanomachine boundary as a reflecting surface that can reflect and obstruct the molecules that are attempting to travel in the opposite direction [34]. We consider the receiving nanomachine boundary as a perfectly absorbing surface; this implies that whenever a signaling molecule hits the boundary of the receiver, it is absorbed by that receiver and contributes to the signal for only one time [34]–[36]. Hence, each molecule only makes a single contribution to the signal [37]. Furthermore, the receiver nanomachine can count the number of molecules per unit time [34], [38]. To send a signal, we assume that the transmitter releases a pulse of Q number of molecules toward the receiver from a point on its surface near the receiver. Based on the absorbed maximum molecules concentration (peak concentration) by the receiver, the receiver detects the signal [39]. Therefore, propagation delay refers to the time between a signal's emission from the transmitter and observation of the signal's peak at the

receiver [35]. We also considered a free diffusion fluidic communication channel with a uniform temperature and viscosity, in which the molecules diffuse freely and propagate through the Brownian motion [40], [41]. Hence, it is possible to achieve bidirectional communication [28]. For two reasons, we considered isomers (such as hexose) as signaling molecules. First, isomers are molecules that have the same *diffusion coefficient*, Ω, but have different chemical properties [42]. Consequently, each isomer denotes a distinct signal and the propagation delay durations of the isomers representing different signaling messages are the same. Moreover, the required number of isomers increases with the increase in the number of D. Second, isomers are generally regarded as being safe in humans [42].

Based on the functions, we consider three types of nanomachines: the *control nanomachine* (C), the *drug-carrying nanomachine* (D), and the *monitoring nanomachine* (M). The C is the internal trigger-source that can coordinate the drug release of D. The D refers to a drug carrier that can release the drug molecules and the signaling molecules when commanded to by the C and the M, respectively. The M is designed to assist the C and the D in measuring the propagation delay. Due to its proximity to the infected site, the M can be used to detect the number of absorbing drug molecules at the infected site. The D is located between the C and the M. Here, we consider two Ds and denote them as D_1 and D_2. We note that the propagation delay between D and the infected site can be approximated by the propagation delay between the D and the M because the M is in close proximity to the infected site. In medical applications, such particular topology configurations are reportedly feasible [43]. d_{x_y} denotes the distances between x and y where $x, y \in \{C, D_1, D_2, M\}$. It is assumed that $d_{C\_D_1} < d_{C\_D_2}$ and $d_{M\_D_1} > d_{M\_D_2}$. This assumption is realistic because of the random positions of the Ds between the C and the M, where some Ds can be close to the C, while some Ds can be close to the M. Therefore, we consider both scenarios.

III. OPERATION OF THE PROPOSED SCHEMES

Two novel SDD schemes are proposed: DTE-SDD and iDTE-SDD schemes to trigger the Ds internally to deliver their drugs to the infected site simultaneously. The C estimates the propagation delay between the D and the M by directly sending a control signal to the M in the DTE-SDD scheme. By contrast, the C sends control signals to the D to estimate the propagation delay between the D and the M in the iDTE-SDD scheme. Both schemes consist of two phases: the *propagation delay estimation phase* and the *simultaneous drug delivery phase*. In the propagation delay estimation phase, the C estimates the propagation delay between the C and the D. Additionally, the C also estimates the propagation delay between the M and the D. In the SDD phase, the C triggers the Ds to release their drugs so that the drugs are delivered at the infected site at the common time T_Σ. The propagation delay between nanomachines x and y is denoted by τ_{x_y}, where $x, y \in \{C, D_i, M\}$ and where $i \in N$ (N is the number of D). τ_{x_y} is the random delay due to the noise produced by the molecule's random motion in the environment. Therefore, τ_{x_y} with noise can be denoted as:

$$\tau_{x\_y} = E[\tau_{x\_y}] + X, \tag{1}$$

where $\mathrm{E}[\tau_{x\_y}]$ is the expectation value of τ_{x_y} and is equal to $\frac{d^2}{6\Omega}$. X is the corresponding propagation delay noise and the random variable with a Gaussian distribution denoted by: [27]

$$X \sim \mathcal{N}(0,\ \sigma^2_{\tau_{x\_y}}), \tag{2}$$

where the mean and variance are 0 and $\sigma^2_{\tau_{x\_y}}$, respectively.

A. DTE-SDD SCHEME

Fig. 2 shows the propagation delay estimation phase and the SDD phase of the DTE-SDD scheme. Table. 2 contains the list of events with their descriptions of the DTE-SDD scheme.

TABLE 2. List of events in DTE-SDD scheme.

Event	Description	Time of event	Record time
Ⓐ	C broadcasts INI	$T_{Ⓐ}$	Yes
Ⓑ	D receives INI and sends RES to C	$T_{Ⓑ}$	No
Ⓒ	C receives RES of D	$T_{Ⓒ}$	Yes
Ⓓ	M receives INI and sends RES to C and D	$T_{Ⓓ}$	No
Ⓔ	C receives RES of M	$T_{Ⓔ}$	Yes
Ⓕ	D receives RES of M and sends RLY to C	$T_{Ⓕ}$	No
Ⓖ	C receives RLY of D	$T_{Ⓖ}$	Yes
Ⓗ	C sends DRR to D	$T_{Ⓗ}$	No
Ⓘ	D receives DRR and releases the drugs	$T_{Ⓘ}$	No
Ⓙ	Infected site receives the drugs	T_Σ	No

1) THE PROPAGATION DELAY ESTIMATION PHASE

C begins the propagation delay estimation by broadcasting the initiation signal INI using Q number of signaling molecules to the D and the M. This event is marked by Ⓐ and the time is denoted by $T_{Ⓐ}$. Therefore, the arrival time of INI at D_i can be written as

$$T_{Ⓑ,D_i} = T_{Ⓐ} + \tau^{Ⓐ}_{C\_D_i}, \tag{3}$$

where the event Ⓑ denotes the arrival of INI at the D. In $\tau^{Ⓐ}_{C\_D_i}$, the superscript notation denotes the signal-sending-time event. On receiving the INI, D_i immediately sends back the response signal, RES_i, which will arrive at $T_{Ⓒ,D_i} = T_{Ⓑ,D_i} + \tau^{Ⓑ}_{C\_D_i}$. The C records $T_{Ⓐ}$ and $T_{Ⓒ,D_i}$. Then, the C can estimate the $\tau_{C\_D_i}$ using the round-trip time as

$$\tilde{\tau}_{C\_D_i} = \frac{T_{Ⓒ,D_i} - T_{Ⓐ}}{2}. \tag{4}$$

The numerator corresponds to the round-trip time between the C and the D, which is divided by 2 as both nanomachines are static with a fixed distance and also because the forward

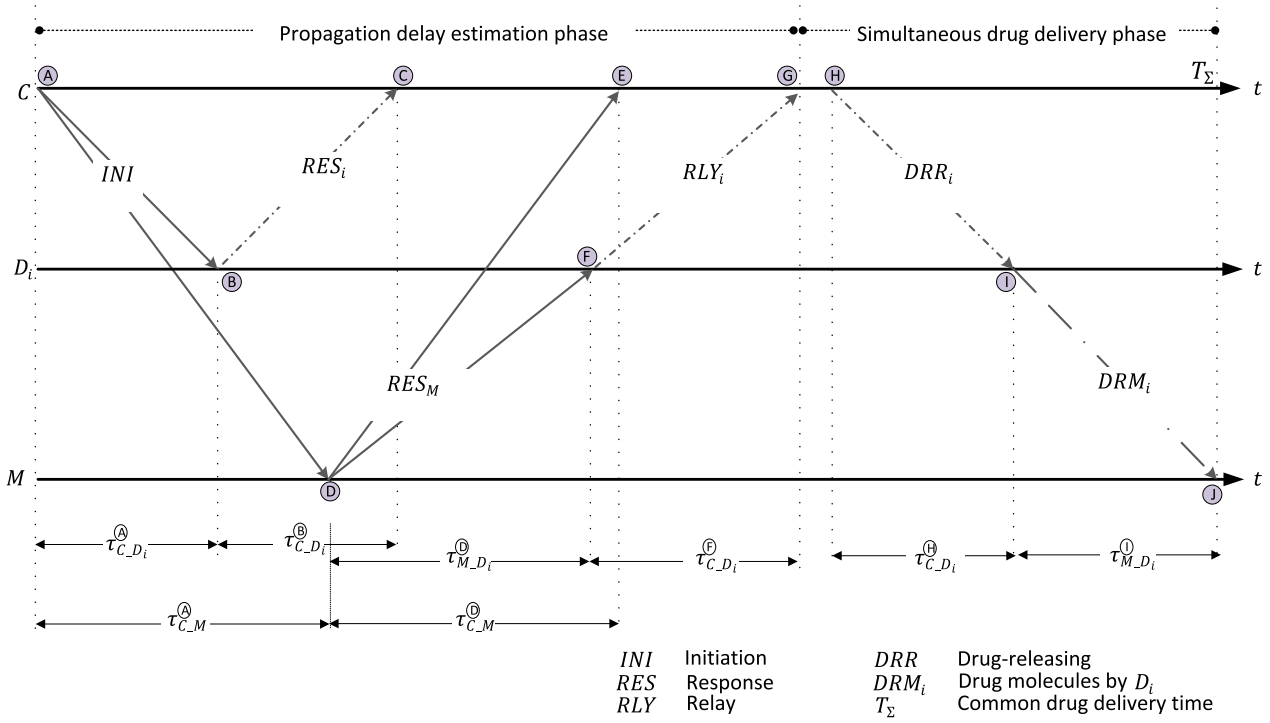

FIGURE 2. Operation of the proposed DTE-SDD scheme.

and backward signal directions are assumed to be identical. Similarly, the arrival time of *INI* at the M (marked as Ⓓ) is

$$T_{Ⓓ} = T_{Ⓐ} + \tau^{Ⓐ}_{C\_M}. \tag{5}$$

Analogously, the M immediately sends back the RES_M toward the C upon receiving the *INI*. Then RES_M arrives (marked as Ⓔ) at $T_{Ⓔ} = T_{Ⓓ} + \tau^{Ⓓ}_{C\_M}$. Similar to (4), the estimated τ_{C_M} is obtained by

$$\tilde{\tau}_{C\_M} = \frac{T_{Ⓔ} - T_{Ⓐ}}{2}. \tag{6}$$

The RES_M is also received by D_i at $T_{Ⓕ,D_i}$ and it immediately sends a relay signal, RLY_i, to C (marked by Ⓕ), which arrives at $T_{Ⓖ,D_i}$ (marked by Ⓖ). Therefore, the round-trip time between the C and the M through D_i is given by:

$$RTT_{C\_D_i\_M} = T_{Ⓖ,D_i} - T_{Ⓐ}. \tag{7}$$

Using $\tilde{\tau}_{C\_D_i}$, $\tilde{\tau}_{C\_M}$, and $RTT_{C\_D_i\_M}$, the C estimates $\tau_{M\_D_i}$ as:

$$\tilde{\tau}_{M\_D_i} = RTT_{C\_D_i\_M} - \tilde{\tau}_{C\_D_i} - \tilde{\tau}_{C\_M}. \tag{8}$$

2) SIMULTANEOUS DRUG-DELIVERY PHASE

To deliver the drugs simultaneously at T_Σ, the C determines the time instant $T_{Ⓗ,D_i}$ at which the C sends a drug-releasing signal, DRR_i, to D_i (marked as Ⓗ) to trigger D_i to release the drug. We note that T_Σ is known to the C. Then,

$$T_{Ⓗ,D_i} = T_\Sigma - \tilde{\tau}_{M\_D_i} - \tilde{\tau}_{C\_D_i}. \tag{9}$$

When the D is triggered by the C, it releases the drug molecules (marked by Ⓘ). Therefore, the drug releasing time of D_i is:

$$T_{Ⓘ,D_i} = T_{Ⓗ,D_i} + \tau^{Ⓗ}_{C\_D_i}. \tag{10}$$

The released drug molecules should arrive at the infected site at T_Σ. However, due to the varying channel conditions and the randomness of molecular movement, the drug molecules may arrive at the infected site in a nonsimultaneous manner. Therefore, the actual drug delivery time of D_i (marked by Ⓙ) denoted by

$$\zeta_{D_i} = T_{Ⓘ,D_i} + \tau^{Ⓘ}_{M\_D_i}, \tag{11}$$

is different from T_Σ.

3) ANALYSIS OF DRUG-DELIVERY ERROR

The drug-delivery-time error is defined as the time difference between the maximum and the minimum delivery times among all the Ds where the total number of D is N. Let i^+ and i^- denote the index for D with the maximum and the minimum drug-delivery times, respectively. We can express it as:

$$\underset{\forall i \in N}{\text{argmax}}\ \zeta_{D_i} \triangleq \zeta_{D_{i^+}},$$

and

$$\underset{\forall i \in N}{\text{argmin}}\ \zeta_{D_i} \triangleq \zeta_{D_{i^-}}. \tag{12}$$

Then the drug-delivery-time error, ε, can be written as:

$$\varepsilon = \zeta_{D_{i^+}} - \zeta_{D_{i^-}}. \tag{13}$$

Applying values from (10) and (11) in (13), we can write (13) as:

$$\varepsilon = T_{\text{Ⓗ},D_{i+}} + \tau^{\text{Ⓗ}}_{C\_D_{i+}} + \tau^{\text{Ⓘ}}_{M\_D_{i+}} - T_{\text{Ⓗ},D_{i-}} - \tau^{\text{Ⓗ}}_{C\_D_{i-}} - \tau^{\text{Ⓘ}}_{M\_D_{i-}}. \quad (14)$$

Using (9), we rearrange (14) as:

$$\varepsilon = T_\Sigma - \tilde{\tau}_{M\_D_{i+}} - \tilde{\tau}_{C\_D_{i+}} + \tau^{\text{Ⓗ}}_{C\_D_{i+}} + \tau^{\text{Ⓘ}}_{M\_D_{i+}} - T_\Sigma + \tilde{\tau}_{M\_D_{i-}} + \tilde{\tau}_{C\_D_{i-}} - \tau^{\text{Ⓗ}}_{C\_D_{i-}} - \tau^{\text{Ⓘ}}_{M\_D_{i-}}. \quad (15)$$

Then, using (8) we can obtain:

$$\begin{aligned}\varepsilon &= -RTT_{C\_D_{i+}\_M} + \tilde{\tau}_{C\_D_{i+}} + \tilde{\tau}_{C\_M} - \tilde{\tau}_{C\_D_{i+}} + \tau^{\text{Ⓗ}}_{C\_D_{i+}} \\ &\quad + \tau^{\text{Ⓘ}}_{M\_D_{i+}} + RTT_{C\_D_{i-}\_M} - \tilde{\tau}_{C\_D_{i-}} - \tilde{\tau}_{C\_M} + \tilde{\tau}_{C\_D_{i-}} \\ &\quad - \tau^{\text{Ⓗ}}_{C\_D_{i-}} - \tau^{\text{Ⓘ}}_{M\_D_{i-}} \\ &= -RTT_{C\_D_{i+}\_M} + \tau^{\text{Ⓗ}}_{C\_D_{i+}} + \tau^{\text{Ⓘ}}_{M\_D_{i+}} + RTT_{C\_D_{i-}\_M} \\ &\quad - \tau^{\text{Ⓗ}}_{C\_D_{i-}} - \tau^{\text{Ⓘ}}_{M\_D_{i-}} \\ &= -\tau^{\text{Ⓓ}}_{M\_D_{i+}} - \tau^{\text{Ⓕ}}_{C\_D_{i+}} + \tau^{\text{Ⓗ}}_{C\_D_{i+}} + \tau^{\text{Ⓘ}}_{M\_D_{i+}} \\ &\quad + \tau^{\text{Ⓓ}}_{M\_D_{i-}} + \tau^{\text{Ⓕ}}_{C\_D_{i-}} - \tau^{\text{Ⓗ}}_{C\_D_{i-}} - \tau^{\text{Ⓘ}}_{M\_D_{i-}}, \end{aligned} \quad (16)$$

where $\tau^{\text{Ⓕ}}_{C\_D_{i+}}$ and $\tau^{\text{Ⓗ}}_{C\_D_{i+}}$ are independent and identically distributed (i.i.d.) random variables with a Gaussian distribution having a mean and a variance of $\mu_{C\_D_{i+}}$ and $\sigma^2_{C\_D_{i+}}$, respectively. Similarly, $\tau^{\text{Ⓓ}}_{M\_D_{i+}}$ and $\tau^{\text{Ⓘ}}_{M\_D_{i+}}$ are i.i.d. random variables with a mean $\mu_{M\_D_{i+}}$ and a variance of $\sigma^2_{M\_D_{i+}}$.

$\tau^{\text{Ⓕ}}_{C\_D_{i-}}$ and $\tau^{\text{Ⓗ}}_{C\_D_{i-}}$ are also i.i.d. random variables with a Gaussian distribution having a mean and a variance of $\mu_{C\_D_{i-}}$ and $\sigma^2_{C\_D_{i-}}$, respectively. Similarly, $\tau^{\text{Ⓓ}}_{M\_D_{i-}}$ and $\tau^{\text{Ⓘ}}_{M\_D_{i-}}$ are i.i.d. with a mean of $\mu_{M\_D_{i-}}$ and a variance of $\sigma^2_{M\_D_{i-}}$. As a result of the Gaussian distribution's summation property, ε is also a Gaussian distributed random variable with a mean of μ_ε and a variance of σ^2_ε, where μ_ε and σ^2_ε can be obtained as: [44], [45]

$$\begin{aligned}\mu_\varepsilon &= -\mu_{M\_D_{i+}} - \mu_{C\_D_{i+}} + \mu_{C\_D_{i+}} + \mu_{M\_D_{i+}} \\ &\quad + \mu_{M\_D_{i-}} + \mu_{C\_D_{i-}} - \mu_{M\_D_{i-}} - \mu_{C\_D_{i-}} \\ &= 0, \end{aligned} \quad (17)$$

and

$$\begin{aligned}\sigma^2_\varepsilon &= \sigma^2_{M\_D_{i+}} + \sigma^2_{C\_D_{i+}} + \sigma^2_{C\_D_{i+}} + \sigma^2_{M\_D_{i+}} \\ &\quad + \sigma^2_{M\_D_{i-}} + \sigma^2_{C\_D_{i-}} + \sigma^2_{M\_D_{i-}} + \sigma^2_{C\_D_{i-}} \\ &= 2\left(\sigma^2_{M\_D_{i+}} + \sigma^2_{C\_D_{i+}} + \sigma^2_{M\_D_{i-}} + \sigma^2_{C\_D_{i-}}\right). \end{aligned} \quad (18)$$

Therefore, due to $\mu_\varepsilon = 0$,

$$\sqrt{E[\varepsilon^2]} = \sigma_\varepsilon, \quad (19)$$

which is the root mean squared error (RMSE).

TABLE 3. List of events in iDTE-SDD scheme.

Event	Description	Time of event	Record time
Ⓐ	C broadcasts INI	$T_{\text{Ⓐ}}$	Yes
Ⓑ	D receives INI and sends RES and INI to C and M, respectively	$T_{\text{Ⓑ}}$	Yes
Ⓒ	C receives RES of D	$T_{\text{Ⓒ}}$	Yes
Ⓓ	M receives INI and sends RES to D	$T_{\text{Ⓓ}}$	No
Ⓔ	D receives RES of M	$T_{\text{Ⓔ}}$	Yes
Ⓕ	C sends EST to D	$T_{\text{Ⓕ}}$	Yes
Ⓖ	D receives EST of C	$T_{\text{Ⓖ}}$	No
Ⓗ	D sends ETR to C	$T_{\text{Ⓗ}}$	No
Ⓘ	C receives ETR	$T_{\text{Ⓘ}}$	Yes
Ⓙ	C sends DRR to D	$T_{\text{Ⓙ}}$	No
Ⓚ	D receives DRR and releases the drugs	$T_{\text{Ⓚ}}$	No
Ⓛ	Infected site receives the drugs	T_Σ	No

B. iDTE-SDD SCHEME

In the following subsection, we will describe the propagation delay estimation phase and the SDD phase of the iDTE-SDD scheme. Table 3 describes the events used in the iDTE-SDD scheme.

1) THE PROPAGATION DELAY ESTIMATION PHASE

Fig. 3 shows that the C starts the propagation delay estimation procedure by transmitting INI at $T_{\text{Ⓐ}}$ using Q number of signaling molecules to D. This event is marked by Ⓐ. INI arrives at D_i (marked by Ⓑ) at $T_{\text{Ⓑ},D_i} = T_{\text{Ⓐ}} + \tau^{\text{Ⓐ}}_{C\_D_i}$.

After receiving INI, D_i immediately sends back RES_i, which will reach at $T_{\text{Ⓒ},D_i}$ (marked as Ⓒ), such that $T_{\text{Ⓒ},D_i} = T_{\text{Ⓑ},D_i} + \tau^{\text{Ⓑ}}_{C\_D_i}$. The C records $T_{\text{Ⓒ},D_i}$ and $T_{\text{Ⓐ}}$. Then, it estimates the propagation delay between the C and D_i as:

$$\tilde{\tau}_{C\_D_i} = \frac{T_{\text{Ⓒ},D_i} - T_{\text{Ⓐ}}}{2} = \frac{\tau^{\text{Ⓐ}}_{C\_D_i} + \tau^{\text{Ⓑ}}_{C\_D_i}}{2}. \quad (20)$$

Additionally, after sending RES_i, D_i immediately sends an INI_i to M to estimate the propagation delay to the infected site. For simplicity, we do not consider the sending time difference between INI_i and RES_i. INI_i arrives at $T_{\text{Ⓓ},D_i}$ (marked by Ⓓ). Therefore, $T_{\text{Ⓓ},D_i} = T_{\text{Ⓑ},D_i} + \tau^{\text{Ⓑ}}_{M\_D_i}$. After receiving INI_i, the M immediately sends back RES_M, which arrives at D_i at $T_{\text{Ⓔ},D_i}$ (marked as Ⓔ). Hence, $T_{\text{Ⓔ},D_i} = T_{\text{Ⓓ},D_i} + \tau^{\text{Ⓓ}}_{M\_D_i}$. The D records $T_{\text{Ⓑ},D_i}$ and $T_{\text{Ⓔ},D_i}$. Finally, the D estimates the round-trip time between the D and the M; this is used to estimate the $\tau_{M\_D_i}$ as:

$$\tilde{\tau}_{M\_D_i} = \frac{T_{\text{Ⓔ},D_i} - T_{\text{Ⓑ},D_i}}{2} = \frac{\tau^{\text{Ⓑ}}_{M\_D_i} + \tau^{\text{Ⓓ}}_{M\_D_i}}{2}. \quad (21)$$

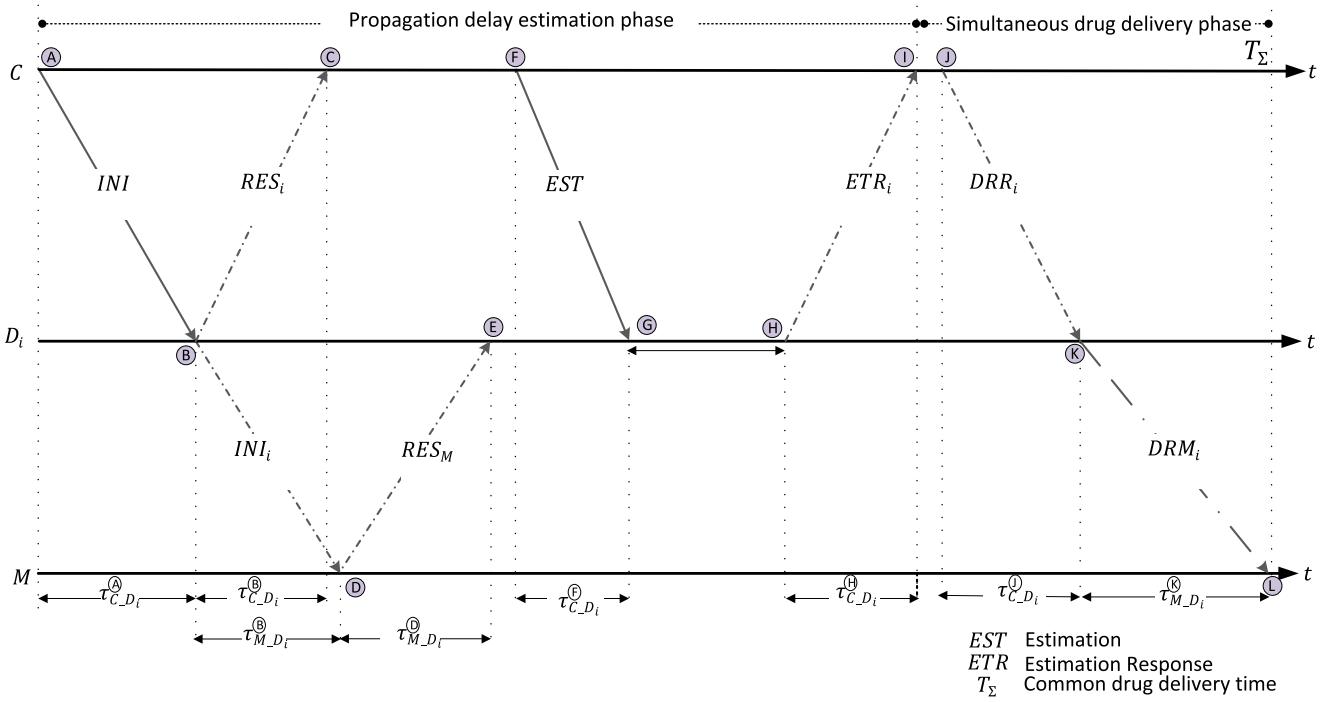

FIGURE 3. Operation of the proposed iDTE-SDD scheme.

The C again sends an estimation signal, EST, to D to estimate the propagation delay between the D and the M at time $T_{\textcircled{F}}$ (marked as Ⓕ), which arrives at $T_{\textcircled{G},D_i} = T_{\textcircled{F}} + \tau^{\textcircled{F}}_{C\_D_i}$ (marked by Ⓖ). On receiving the EST, the D sends back an estimation response signal, ETR_i, after time $\tilde{\tau}_{M\_D_i}$ at $T_{\textcircled{H},D_i}$ (marked by Ⓗ). Therefore, $T_{\textcircled{H},D_i} = T_{\textcircled{G},D_i} + \tilde{\tau}_{M\_D_i}$. ETR_i arrives at $T_{\textcircled{I},D_i}$ (marked by Ⓘ). Thereby, $T_{\textcircled{I},D_i} = T_{\textcircled{H},D_i} + \tau^{\textcircled{H}}_{C\_D_i}$. Finally, C estimates the $\tau_{M\_D_{iC}}$ as

$$\begin{aligned}\tilde{\tau}_{M\_D_{iC}} &= T_{\textcircled{I},D_i} - T_{\textcircled{F}} - 2\tilde{\tau}_{C\_D_i} \\ &= \tau^{\textcircled{F}}_{C\_D_i} + \tilde{\tau}_{M\_D_i} + \tau^{\textcircled{H}}_{C\_D_i} - 2\tilde{\tau}_{C\_D_i}, \end{aligned} \tag{22}$$

where $\tilde{\tau}_{M\_D_{iC}}$ is the propagation delay between the M and the D_i, which is estimated by the C.

2) SIMULTANEOUS DRUG-DELIVERY PHASE

After obtaining $\tilde{\tau}_{M\_D_{iC}}$ and $\tilde{\tau}_{C\_D_i}$, the C determines the time instants $T_{\textcircled{J},D_i}$ at which it sends DRR_i (marked by Ⓙ) to D_i to trigger the D_i to release their drugs which can be obtained as:

$$T_{\textcircled{J},D_i} = T_\Sigma - \tilde{\tau}_{M\_D_{iC}} - \tilde{\tau}_{C\_D_i}. \tag{23}$$

The DRR_i arrives at $T_{\textcircled{K},D_i}$ (marked by Ⓚ), and the actual drug-delivery time (marked by Ⓛ) can be obtained as:

$$\zeta_{D_i} = T_{\textcircled{J},D_i} + \tau^{\textcircled{J}}_{C\_D_i} + \tau^{\textcircled{K}}_{M\_D_i}. \tag{24}$$

3) ANALYSIS OF DRUG-DELIVERY ERROR

Using the same definition of $\zeta_{D_{i^+}}$, $\zeta_{D_{i^-}}$, and ε as DTE-SDD,

$$\begin{aligned}\varepsilon &= \zeta_{D_{i^+}} - \zeta_{D_{i^-}} \\ &= T_{\textcircled{J},D_{i^+}} + \tau^{\textcircled{J}}_{C\_D_{i^+}} + \tau^{\textcircled{K}}_{M\_D_{i^+}} - T_{\textcircled{J},D_{i^-}} \\ &\quad - \tau^{\textcircled{J}}_{C\_D_{i^-}} - \tau^{\textcircled{K}}_{M\_D_{i^-}}. \end{aligned} \tag{25}$$

Again, applying values from (23), we obtain in (25)

$$\begin{aligned}\varepsilon &= \left(T_\Sigma - \tilde{\tau}_{C\_D_{i^+}} - \tilde{\tau}_{M\_D_{i^+C}}\right) + \tau^{\textcircled{J}}_{C\_D_{i^+}} + \tau^{\textcircled{K}}_{M\_D_{i^+}} \\ &\quad - \left(T_\Sigma - \tilde{\tau}_{C\_D_{i^-}} - \tilde{\tau}_{M\_D_{i^-C}}\right) - \tau^{\textcircled{J}}_{C\_D_{i^-}} - \tau^{\textcircled{K}}_{M\_D_{i^-}}. \end{aligned} \tag{26}$$

Applying (22) in (26), we set (26) as:

$$\begin{aligned}\varepsilon &= -\tau^{\textcircled{F}}_{C\_D_{i^+}} - \tilde{\tau}_{M\_D_{i^+}} - \tau^{\textcircled{H}}_{C\_D_{i^+}} + 2\tilde{\tau}_{C\_D_{i^+}} - \tilde{\tau}_{C\_D_{i^+}} \\ &\quad + \tau^{\textcircled{J}}_{C\_D_{i^+}} + \tau^{\textcircled{K}}_{M\_D_{i^+}} + \tau^{\textcircled{F}}_{C\_D_{i^-}} + \tilde{\tau}_{M\_D_{i^-}} + \tau^{\textcircled{H}}_{C\_D_{i^-}} \\ &\quad - 2\tilde{\tau}_{C\_D_{i^-}} + \tilde{\tau}_{C\_D_{i^-}} - \tau^{\textcircled{J}}_{C\_D_{i^-}} - \tau^{\textcircled{K}}_{M\_D_{i^-}}. \end{aligned} \tag{27}$$

From (20) and (21), we get in (27):

$$\begin{aligned}\varepsilon &= -\tau^{\textcircled{F}}_{C\_D_{i^+}} - \left(\frac{\tau^{\textcircled{B}}_{M\_D_{i^+}} + \tau^{\textcircled{D}}_{M\_D_{i^+}}}{2}\right) - \tau^{\textcircled{H}}_{C\_D_{i^+}} \\ &\quad + \frac{1}{2}\tau^{\textcircled{A}}_{C\_D_{i^+}} + \frac{1}{2}\tau^{\textcircled{B}}_{C\_D_{i^+}} + \tau^{\textcircled{J}}_{C\_D_{i^+}} + \tau^{\textcircled{K}}_{M\_D_{i^+}} \\ &\quad + \tau^{\textcircled{F}}_{C\_D_{i^-}} + \left(\frac{\tau^{\textcircled{B}}_{M\_D_{i^-}} + \tau^{\textcircled{D}}_{M\_D_{i^-}}}{2}\right) + \tau^{\textcircled{H}}_{C\_D_{i^-}} \\ &\quad - \frac{1}{2}\tau^{\textcircled{A}}_{C\_D_{i^-}} - \frac{1}{2}\tau^{\textcircled{B}}_{C\_D_{i^-}} - \tau^{\textcircled{J}}_{C\_D_{i^-}} - \tau^{\textcircled{K}}_{M\_D_{i^-}}. \end{aligned} \tag{28}$$

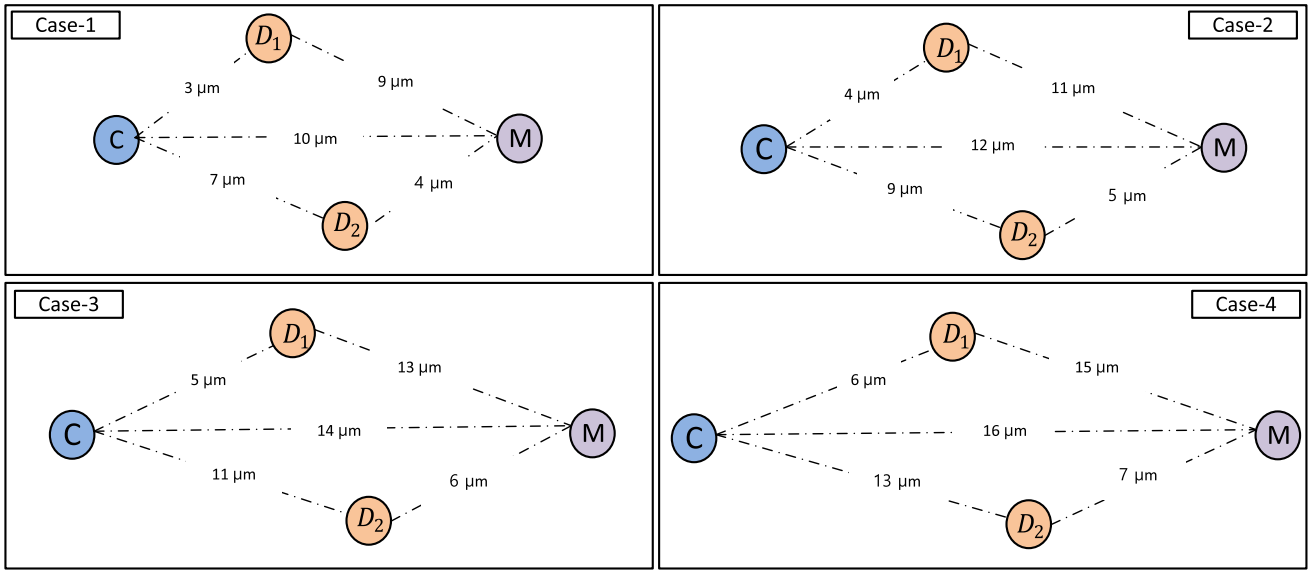

FIGURE 4. Illustrations of four cases.

In the same way as in the DTE-SDD system, all the propagation delays, $\tau^{(z)}_{x\_y}$, for different events z, are i.i.d. random variables with a Gaussian distribution mean of μ_{x_y} and a variance of $\sigma^2_{x\_y}$. Therefore, the mean and variance of ε can be written as

$$\begin{aligned}\mu_\varepsilon &= -\mu_{C\_D_{i^+}} - \left(\frac{\mu_{M\_D_{i^+}} + \mu_{M\_D_{i^+}}}{2}\right) - \mu_{C\_D_{i^+}} \\ &\quad + \frac{1}{2}\mu_{C\_D_{i^+}} + \frac{1}{2}\mu_{C\_D_{i^+}} + \mu_{C\_D_{i^+}} + \mu_{M\_D_{i^+}} \\ &\quad + \mu_{C\_D_{i^-}} + \left(\frac{\mu_{M\_D_{i^-}} + \mu_{M\_D_{i^-}}}{2}\right) + \mu_{C\_D_{i^-}} \\ &\quad - \frac{1}{2}\mu_{C\_D_{i^-}} - \frac{1}{2}\mu_{C\_D_{i^-}} - \mu_{C\_D_{i^-}} - \mu_{M\_D_{i^-}} \\ &= -2\mu_{C\_D_{i^+}} + 2\mu_{C\_D_{i^+}} - \mu_{M\_D_{i^+}} + \mu_{M\_D_{i^+}} \\ &\quad - 2\mu_{C\_D_{i^-}} + 2\mu_{C\_D_{i^-}} - \mu_{M\_D_{i^-}} + \mu_{M\_D_{i^-}} \\ &= 0, \end{aligned} \tag{29}$$

and

$$\begin{aligned}\sigma^2_\varepsilon &= \sigma^2_{C\_D_{i^+}} + \left(\frac{\sigma^2_{M\_D_{i^+}} + \sigma^2_{M\_D_{i^+}}}{2}\right) + \sigma^2_{C\_D_{i^+}} \\ &\quad + \frac{1}{2}\sigma^2_{C\_D_{i^+}} + \frac{1}{2}\sigma^2_{C\_D_{i^+}} + \sigma^2_{C\_D_{i^+}} + \sigma^2_{M\_D_{i^+}} \\ &\quad + \sigma^2_{C\_D_{i^-}} + \left(\frac{\sigma^2_{M\_D_{i^-}} + \sigma^2_{M\_D_{i^-}}}{2}\right) + \sigma^2_{C\_D_{i^-}} \\ &\quad + \frac{1}{2}\sigma^2_{C\_D_{i^-}} + \frac{1}{2}\sigma^2_{C\_D_{i^-}} + \sigma^2_{C\_D_{i^-}} + \sigma^2_{M\_D_{i^-}} \\ &= \frac{7}{2}\left(\sigma_{C\_D_{i^+}} + \sigma_{C\_D_{i^-}}\right) + \frac{3}{2}\left(\sigma_{M\_D_{i^+}} + \sigma_{M\_D_{i^-}}\right). \end{aligned} \tag{30}$$

Due to $\mu_\varepsilon = 0$, the RMSE is

$$\begin{aligned}\sqrt{E[\varepsilon^2]} &= \sqrt{\sigma^2_\varepsilon + \mu^2_\varepsilon} \\ &= \sigma_\varepsilon. \end{aligned} \tag{31}$$

IV. NUMERICAL ANALYSIS

The proposed DTE-SDD and iDTE-SDD systems are numerically analyzed in this section. We built a network simulator using the well-recognized MolecUlar CommunicatIoN (MUCIN) simulator [46]. In MUCIN, we performed 6×10^3 simulation replications to generate the dataset for the propagation delays of a signal. We obtained the propagation delay variance using MATLAB's built-in function. We considered the sampling step time $\Delta t = 0.001$ s. The nanomachines' radius r was set to 10 μm [47], the number of D was set to 2, and the diffusion coefficient Ω was set to 597.25 $\mu m^2/s$ [42]. Additionally, we considered different distance values of the nanomachines to evaluate the proposed schemes' performances, as shown in Fig. 4. The evaluation metrics were the RMSE of ε, the cumulative distribution function (CDF) of ε, the drug-delivery time of the Ds, and the energy consumption.

We chose the two-way message exchange-based coordination scheme as a comparison scheme to show that the drug-delivery time could be coordinated without timestamps and also to analyze whether minimizing the perturbation problem (which is the target of [27]) could reduce the delivery-time errors. In [27], a transmitter nanomachine sends a signal toward the receiver nanomachine to achieve coordination with the receiver nanomachine. The receiver nanomachine sends back its timestamp to the transmitter nanomachine after receiving the signal. The transmitter nanomachine uses the timestamp information to measure the perturbations and coordinates with the receiver nanomachine. They exchange R rounds of timestamped signals to improve the estimation accuracy. For fairness of comparison, we added a timestamp signal in [27] to inform the receiver when the drugs would be released. We noted that to make comparisons with our system model, the C and the D were,

respectively, the transmitter and receiver nanomachine. Additionally, in [27], the M is used to obtain the number of absorbed drug molecules.

A. RMSE ANALYSIS

In the computer simulation, the RMSE of ε is obtained by:

$$RMSE = \sqrt{\frac{\sum_{k=1}^{P} \varepsilon^2(k)}{P}}, \tag{32}$$

where $\varepsilon(k)$ is the delivery-time error of the k^{th} replication, and P is the number of simulation replications where $P = 6 \times 10^3$.

Fig. 5 shows the RMSE of the ε versus distances for different cases. We observe that the RMSE in the iDTE-SDD scheme is comparatively lower than that in the DTE-SDD scheme. This is because in the DTE-SDD scheme the C communicates directly with the M, and the d_{C_M} is the largest distance among the other signal distances. As expected in MC, the receiver at a larger distance obtains fewer molecules, increasing the noise in the receiver-measured concentration. Consequently, this noise affects the propagation delay variance, making the RMSE larger. We also observe that the proposed schemes exhibit a smaller RMSE than in [27]. The common point is that the RMSE increases when the distance increases. Furthermore, the results of the proposed schemes' simulation results match their analytical results, validating the correctness of their analytical model.

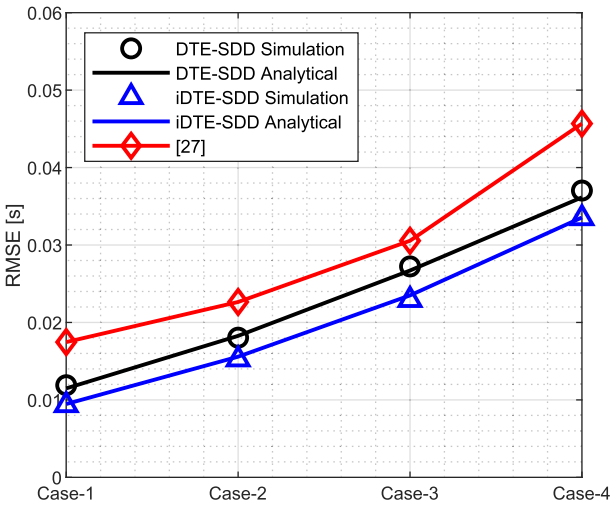

FIGURE 5. RMSE versus d where $Q = 5,000$ molecules.

Fig. 6 shows the RMSE versus Q while considering the distances at Case-2. As expected, it can be seen that the RMSE decreases with the increasing Q. When Q increases, the noise in the received-molecules concentration at the receiver reduces because the receiver receives more molecules, reducing the propagation delay variances that make the RMSE lower. We can also observe that all the schemes show the same trends for all Q, where the iDTE-SDD and the DTE-SDD schemes exhibit a smaller RMSE than in [27]. Therefore,

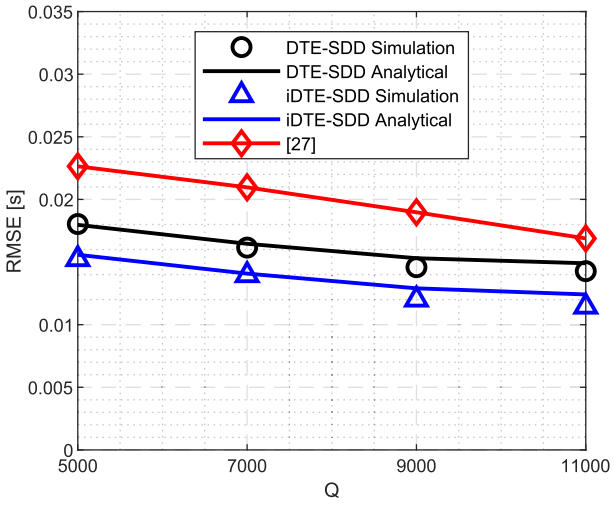

FIGURE 6. RMSE versus Q for Case-2 where $Q = [5,000\ 7,000\ 9,000\ 11,000]$.

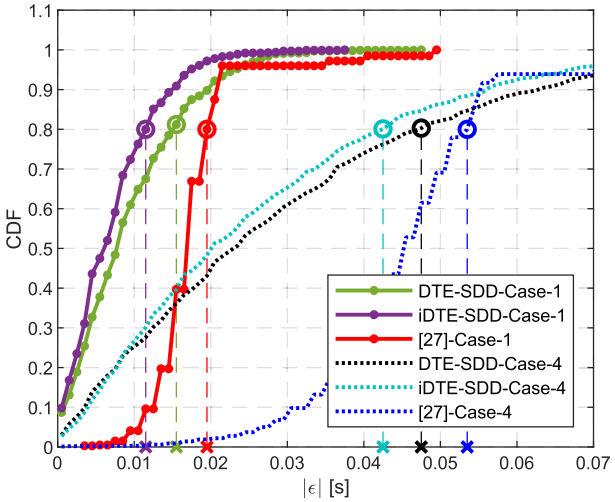

FIGURE 7. CDF of $|\varepsilon|$ where $Q = 5,000$ molecules for Case-1 and Case-4. Here, $|.|$ stands for the absolute operator.

the lower RMSE in the proposed schemes could be beneficial in achieving a highly precise SDD.

B. CDF ANALYSIS

Fig. 7 illustrates the CDF of the absolute value of ε for Case-1 and Case-4 when $Q = 5,000$. We note that Case-4 represents the largest distance between the nanomachines, while Case-1 represents the smallest. The proposed schemes' CDFs show a lower $|\varepsilon|$ for both cases than in [27]. We observe that approximately 80% of the $|\varepsilon|$ values (marked by the circles) are 0.0115 s (marked by the purple 'x'), 0.0153 s (marked by the green 'x'), and 0.0212 s (marked by the red 'x') for iDTE-SDD, the DTE-SDD, and comparison scheme, respectively for Case-1. These values are almost 0.0428 s (marked by the cyan 'x'), 0.0475 s (marked by the black 'x'), and 0.0535 s (marked by the blue 'x') in the iDTE-SDD,

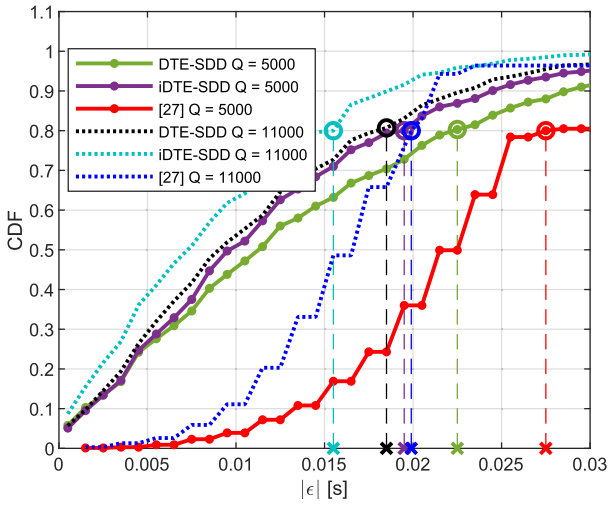

FIGURE 8. CDF of $|\varepsilon|$ for Case-2 where $Q = [5,000\ 11,000]$ molecules.

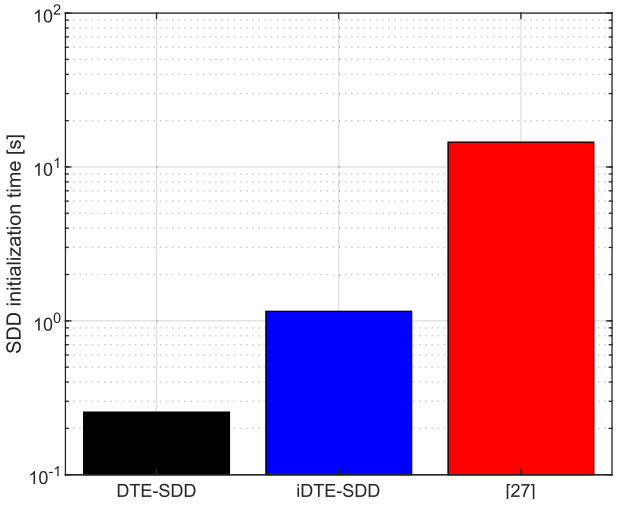

FIGURE 9. SDD initialization time for Case-2 where $Q = 5,000$ molecules.

the DTE-SDD, and [27], respectively for Case-4. From the analysis of the 80% error, it can be seen that the comparison scheme has a large $|\varepsilon|$ because the accuracy of the perturbations' calculation seems to be affected by the propagation delay and its variations. Therefore, estimation alone of the perturbations may be less successful for coordination among the nanomachines than previously thought. The efficiency of such a mechanism of [27] would necessitate prior knowledge of the propagation delay statistical standard deviation, adding to the computational complexity.

In Fig. 8, we illustrate the CDF of $|\varepsilon|$ for different values of Q for Case-2. Almost 80% of the $|\varepsilon|$ values (marked by the circles in the figure) are 0.0195 s (marked by purple the 'x'), 0.0225 s (marked by the green 'x'), and 0.0275 s (marked by the red 'x') in the iDTE-SDD scheme, the DTE-SDD scheme, and [25], respectively for $Q = 5,000$. In comparison, these values are 0.0155 s (marked by the cyan 'x'), 0.0185 s (marked by the black 'x'), and 0.0195 s (marked by blue the 'x') for iDTE-SDD, DTE-SDD, and comparison scheme, respectively for $Q = 11,000$. Therefore, based on the $|\varepsilon|$ values, the proposed schemes exhibit less error and converge to 1 earlier than the comparison scheme, implying that the proposed schemes can better simultaneously deliver drugs at the infected site with minimal $|\varepsilon|$ than the comparison scheme. We can also see that as Q increases, the convergence to 1 increases rapidly because the larger number of emitted molecules can reduce noise and accordingly reduce the propagation delay variances.

C. DRUG-DELIVERY TIME ANALYSIS

Fig. 9 shows the time required to initialize the SDD for each system. The SDD initialization time is the time taken for a system to prepare for drug-delivery, during which the controller performs the estimation of delays or perturbations. We observe that the SDD initialization time is shorter in the DTE-SDD scheme than in the iDTE-SDD scheme. This is because the iDTE-SDD scheme takes longer to estimate the propagation delay than the DTE-SDD scheme. By contrast, the SDD initialization time is higher in [27] than in the proposed schemes. This is because [27] takes longer to exchange the R rounds of the timestamped signal. Therefore, the proposed schemes can simultaneously deliver the drug to the infected site more simply and faster than the comparison scheme.

D. ENERGY COST ANALYSIS

We derived the energy cost from the energy model given in [48], [49]. We refer the reader to [48], [49] for more details. Reference [23] reproduces the energy cost model ((16) in [23]). Therefore, the total energy cost can be defined by:

$$E_{cost} = K \times n \times E_{ps}, \tag{33}$$

where K, n, and E_{ps} are the number of bits in each signal, the number of signal exchanges among the nanomachines, and the energy consumption required to synthesize, transport, and release Q number of molecules, respectively. The values of n is $(2 + 3N)$, $(2 + 5N)$, and $(R(N + 1) + 1)$ are for the DTE-SDD, the iDTE-SDD, and the comparison scheme, respectively, where, N and R are the number of Ds and the number of rounds for exchanging the signals, respectively. The value of $R = 30$ in the comparison scheme [27], while, $R = 1$ in the proposed schemes. All the variables values in (33) are the same as those in [48], [49].

Fig.10 shows the E_{cost} versus the N where $N = [2, 4, 6, 8]$. As expected, the E_{cost} increases when N increases. This is because when N increases, the number of n also increases. However, due to a large number of n in the comparison scheme, its E_{cost} increases drastically. The E_{cost} is lower in the proposed schemes. This is because of the much lower number of n required by the proposed schemes. The E_{cost} in the DTE-SDD scheme is lower than that in the iDTE-SDD

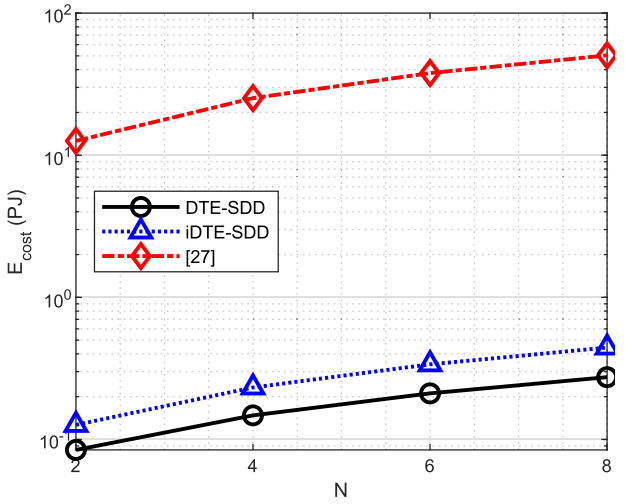

FIGURE 10. Energy cost versus number of drug-carrying nanomachine, N. Here 1 $J = 10^{-12}$ PJ.

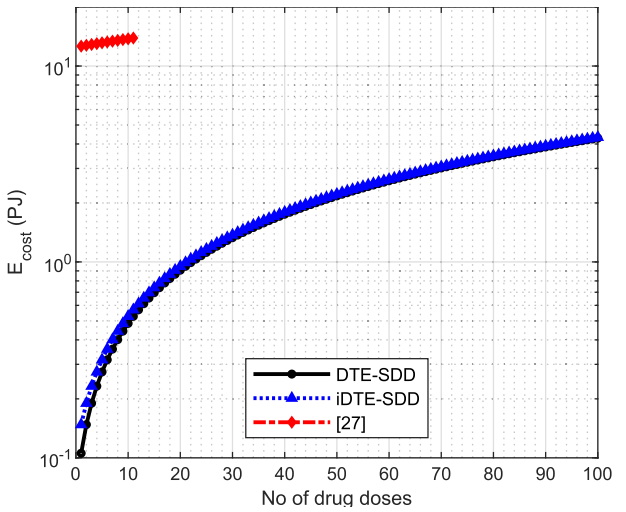

FIGURE 11. Energy cost versus the number of drug doses where $N = 2$.

scheme due to the lower number of n in the DTE-SDD scheme. We found that, on average, the DTE-SDD and iDTE-SDD scheme's E_{cost} were approximately 95% and 94% lower than that of the comparison scheme, respectively. Similarly, the DTE-SDD scheme exhibited an approximately 33% less E_{cost} than the iDTE-SDD scheme. Therefore, among the three schemes, the DTE-SDD scheme was found to be the most energy-efficient.

Fig.11 shows the E_{cost} versus the number of drug doses. Here, in each dose, each D released 5, 000 drug molecules. We assumed that all the systems had the same energy budget, which was 14 PJ. We observed that the number of drug doses was fewer in the comparison scheme than in the proposed schemes. This was because the comparison scheme required more signaling exchanges in the SDD initialization time, resulting in a higher E_{cost}. Therefore, the comparison scheme could achieve 11 drug doses. After 11 doses, the comparison scheme had spent the entire energy budget; therefore, it could not deliver any more drugs to the infected site. By contrast, we found that the numbers of the DTE-SDD and iDTE-SDD schemes' doses could be as high as 329 and 328, respectively. However, to avoid compression of the x-axes, the number of drug doses is shown to 100. Therefore, the proposed schemes could increase the number of drug doses by approximately 30 times. The iDTE-SDD scheme required higher energy than the DTE-SDD scheme due to the longer SDD initialization time. Additionally, for each drug dose, the E_{cost} were the same for the proposed schemes, while the E_{cost} was higher in the comparison scheme, making the proposed schemes more energy-efficient, leading to an increased number of drug doses.

V. CONCLUSION

This paper presented two internally controlled MC-based SDD schemes to reduce the delivery-time error at the infected site for the MC-based TDD system. Based on the propagation delay estimation approach, we proposed: the direct trigger estimate SDD (DTE-SDD) scheme and the indirect trigger estimate SDD (iDTE-SDD) scheme. We derived the analytical error model for simultaneous delivery-time error for both schemes. Simulation results reveal that the DTE-SDD scheme is less complicated and more energy-efficient than the iDTE-SDD scheme, while the iDTE-SDD scheme exhibits a lower delivery-time error in terms of distances and released molecules. Additionally, the proposed schemes outperform a timestamp-based coordination scheme in minimizing the delivery-time error.

Our future work will consider the efficacy of the drug at the infected site by analyzing the effect of the delivery-time error on the maintenance of the TI (LEC or MSC) at the infected site. Additionally, it will involve the reduction of the toxicity of the drugs in healthy cells. The main challenge will be to control the drug-carrying nanomachines that are far away from the infected site. The drug molecules may, therefore, in these cases, diffuse away from the infected area and be absorbed by the healthy cells. Hence, our future goal is to develop an internal controller nanomachine-based energy-efficient and minimally complex TDD system to control the drug release type of drug-carrying nanomachines based on their distance from the infected site.

REFERENCES

[1] I. F. Akyildiz, F. Brunetti, and C. Blázquez, "Nanonetworks: A new communication paradigm," *Comput. Netw.*, vol. 52, no. 12, pp. 2260–2279, Aug. 2008.
[2] T. Nakano, M. J. Moore, F. Wei, A. V. Vasilakos, and J. Shuai, "Molecular communication and networking: Opportunities and challenges," *IEEE Trans. Nanobiosci.*, vol. 11, no. 2, pp. 135–148, Jun. 2012.
[3] V. Loscrí, C. Marchal, N. Mitton, G. Fortino, and A. V. Vasilakos, "Security and privacy in molecular communication and networking: Opportunities and challenges," *IEEE Trans. Nanobiosci.*, vol. 13, no. 3, pp. 198–207, Sep. 2014.
[4] T. Nakano, T. Suda, Y. Okaie, M. J. Moore, and A. V. Vasilakos, "Molecular communication among biological nanomachines: A layered architecture and research issues," *IEEE Trans. Nanobiosci.*, vol. 13, no. 3, pp. 169–197, Sep. 2014.

[5] S. Hiyama, Y. Moritani, T. Suda, R. Egashira, A. Enomoto, M. Moore, and T. Nakano, "Molecular communication," in *Proc. NSTI Nanotechnol. Conf. Trade Show*, vol. 3, 2005, pp. 391–394.

[6] I. Akyildiz, F. Fekri, R. Sivakumar, C. Forest, and B. Hammer, "Monaco: Fundamentals of molecular nano-communication networks," *IEEE Wireless Commun.*, vol. 19, no. 5, pp. 12–18, Oct. 2012.

[7] K. Aghababaiyan, V. Shah-Mansouri, and B. Maham, "Asynchronous neuro-spike array–based communication," in *Proc. IEEE Int. Black Sea Conf. Commun. Netw. (BlackSeaCom)*, Jun. 2018, pp. 1–5.

[8] Ankit and M. R. Bhatnagar, "Boolean AND and OR logic for cell signalling gateways: A communication perspective," *IET Nanobiotechnol.*, vol. 12, no. 8, pp. 1130–1139, Dec. 2018.

[9] U. A. K. Chude-Okonkwo, R. Malekian, B. T. Maharaj, and A. V. Vasilakos, "Molecular communication and nanonetwork for targeted drug delivery: A survey," *IEEE Commun. Surveys Tuts.*, vol. 19, no. 4, pp. 3046–3096, May 2017.

[10] L. Felicetti, M. Femminella, G. Reali, and P. Liò, "Applications of molecular communications to medicine: A survey," *Nano Commun. Netw.*, vol. 7, pp. 27–45, Mar. 2016.

[11] Y. Chahibi, "Molecular communication for drug delivery systems: A survey," *Nano Commun. Netw.*, vol. 11, pp. 90–102, Mar. 2017.

[12] T. Nakano, M. J. Moore, Y. Okaie, A. Enomoto, and T. Suda, "Cooperative drug delivery through molecular communication among biological nanomachines," in *Proc. IEEE Int. Conf. Commun. Workshops (ICC)*, Jun. 2013, pp. 809–812.

[13] Y. Chahibi, M. Pierobon, S. O. Song, and I. F. Akyildiz, "A molecular communication system model for particulate drug delivery systems," *IEEE Trans. Biomed. Eng.*, vol. 60, no. 12, pp. 3468–3483, Dec. 2013.

[14] M. Femminella, G. Reali, and A. V. Vasilakos, "A molecular communications model for drug delivery," *IEEE Trans. Nanobiosci.*, vol. 14, no. 8, pp. 935–945, Dec. 2015.

[15] L. Felicetti, M. Femminella, G. Reali, T. Nakano, and A. V. Vasilakos, "TCP-like molecular communications," *IEEE J. Sel. Areas Commun.*, vol. 32, no. 12, pp. 2354–2367, Dec. 2014.

[16] T. Nakano, Y. Okaie, and A. V. Vasilakos, "Transmission rate control for molecular communication among biological nanomachines," *IEEE J. Sel. Areas Commun.*, vol. 31, no. 12, pp. 835–846, Dec. 2013.

[17] B. P. Timko, T. Dvir, and D. S. Kohane, "Remotely triggerable drug delivery systems," *Adv. Mater.*, vol. 22, no. 44, pp. 4925–4943, Nov. 2010.

[18] A. Wicki, D. Witzigmann, V. Balasubramanian, and J. Huwyler, "Nanomedicine in cancer therapy: Challenges, opportunities, and clinical applications," *J. Controlled Release*, vol. 200, pp. 138–157, Feb. 2015.

[19] C. Li, J. Wang, Y. Wang, H. Gao, G. Wei, Y. Huang, H. Yu, Y. Gan, Y. Wang, L. Mei, H. Chen, H. Hu, Z. Zhang, and Y. Jin, "Recent progress in drug delivery," *Acta Pharmaceutica Sinica B*, vol. 9, no. 6, pp. 1145–1162, 2019.

[20] M. Biletic, F. H. Juwono, and L. Gopal, "Nanonetworks and molecular communications for biomedical applications," *IEEE Potentials*, vol. 39, no. 3, pp. 25–30, May 2020.

[21] L. Tang, A. L. van de Ven, D. Guo, V. Andasari, V. Cristini, K. C. Li, and X. Zhou, "Computational modeling of 3D tumor growth and angiogenesis for chemotherapy evaluation," *PLoS ONE*, vol. 9, no. 1, pp. 1–12, 2014.

[22] S. Salehi, N. S. Moayedian, S. S. Assaf, R. G. Cid-Fuentes, J. Solé-Pareta, and E. Alarcón, "Releasing rate optimization in a single and multiple transmitter local drug delivery system with limited resources," *Nano Commun. Netw.*, vol. 11, pp. 114–122, Mar. 2017.

[23] T. Islam, E. Shitiri, and H.-S. Cho, "A simultaneous drug release scheme for targeted drug delivery using molecular communications," *IEEE Access*, vol. 8, pp. 91770–91778, 2020.

[24] P. Y. Muller and M. N. Milton, "The determination and interpretation of the therapeutic index in drug development," *Nature Rev. Drug Discovery*, vol. 11, no. 10, pp. 751–761, Oct. 2012.

[25] L. McCallum, S. Lip, and S. Padmanabhan, "Pharmacodynamic pharmacogenomics," in *Handbook of Pharmacogenomics and Stratified Medicine*, S. Padmanabhan, Ed. San Diego, CA, USA: Academic, 2014, ch. 8, pp. 365–383.

[26] L. Felicetti, M. Femminella, and G. Reali, "Congestion control in molecular cyber-physical systems," *IEEE Access*, vol. 5, pp. 10000–10011, 2017.

[27] L. Lin, C. Yang, M. Ma, S. Ma, and H. Yan, "A clock synchronization method for molecular nanomachines in bionanosensor networks," *IEEE Sensors J.*, vol. 16, no. 19, pp. 7194–7203, Oct. 2016.

[28] L. Lin, C. Yang, and M. Ma, "Offset and skew estimation for clock synchronization in molecular communication systems," in *Proc. 9th EAI Int. Conf. Bio-Inspired Inf. Commun. Technol. (BIONETICS)*, 2016, pp. 152–156.

[29] E. Shitiri, H. B. Yilmaz, and H.-S. Cho, "A time-slotted molecular communication (TS-MOC): Framework and time-slot errors," *IEEE Access*, vol. 7, pp. 78146–78158, 2019.

[30] I. Llatser, A. Cabellos-Aparicio, M. Pierobon, and E. Alarcon, "Detection techniques for diffusion-based molecular communication," *IEEE J. Sel. Areas Commun.*, vol. 31, no. 12, pp. 726–734, Dec. 2013.

[31] A. Noel, D. Makrakis, and A. Hafid, "Channel impulse responses in diffusive molecular communication with spherical transmitters," in *Proc. 28th Biennial Symp. Commun. Program (BSC)*, Jun. 2016. [Online]. Available: http://infotheory.ca/bsc2016/wp-content/uploads/2016/02/Final-Program-BSC16.pdf

[32] Y. Fang, A. Noel, N. Yang, A. W. Eckford, and R. A. Kennedy, "Symbol-by-symbol maximum likelihood detection for cooperative molecular communication," *IEEE Trans. Commun.*, vol. 67, no. 7, pp. 4885–4899, Jul. 2019.

[33] S. Salehi, N. S. Moayedian, S. H. Javanmard, and E. Alarcón, "Lifetime improvement of a multiple transmitter local drug delivery system based on diffusive molecular communication," *IEEE Trans. Nanobiosci.*, vol. 17, no. 3, pp. 352–360, Jul. 2018.

[34] H. B. Yilmaz, G.-Y. Suk, and C.-B. Chae, "Chemical propagation pattern for molecular communications," *IEEE Wireless Commun. Lett.*, vol. 6, no. 2, pp. 226–229, Apr. 2017.

[35] H. B. Yilmaz, A. C. Heren, T. Tugcu, and C.-B. Chae, "Three-dimensional channel characteristics for molecular communications with an absorbing receiver," *IEEE Commun. Lett.*, vol. 18, no. 6, pp. 929–932, Jun. 2014.

[36] A. Noel, Y. Deng, D. Makrakis, and A. Hafid, "Active versus passive: Receiver model transforms for diffusive molecular communication," in *Proc. IEEE Global Commun. Conf. (GLOBECOM)*, Dec. 2016, pp. 1–6.

[37] J. W. Kwack, H. B. Yilmaz, N. Farsad, C.-B. Chae, and A. Goldsmith, "Two way molecular communications," in *Proc. 5th ACM Int. Conf. Nanosc. Comput. Commun. (NANOCOM)*. New York, NY, USA: ACM, 2018, pp. 1–5.

[38] H. B. Yilmaz and C.-B. Chae, "Simulation study of molecular communication systems with an absorbing receiver: Modulation and ISI mitigation techniques," *Simul. Model. Pract. Theory*, vol. 49, pp. 136–150, Dec. 2014.

[39] M. S. Kuran, H. B. Yilmaz, T. Tugcu, and I. F. Akyildiz, "Modulation techniques for communication via diffusion in nanonetworks," in *Proc. IEEE Int. Conf. Commun. (ICC)*, Jun. 2011, pp. 1–5.

[40] G. D. Ntouni, V. M. Kapinas, and G. K. Karagiannidis, "On the optimal timing of detection in molecular communication systems," in *Proc. 24th Int. Conf. Telecommun. (ICT)*, May 2017, pp. 1–5.

[41] A. Einstein, *Investigations on the Brownian Movement*, vol. 322, no. 8. New York, NY, USA: Dover, 1956, pp. 549–560.

[42] N.-R. Kim and C.-B. Chae, "Novel modulation techniques using isomers as messenger molecules for nano communication networks via diffusion," *IEEE J. Sel. Areas Commun.*, vol. 31, no. 12, pp. 847–856, Dec. 2013.

[43] Y. Fang, A. Noel, N. Yang, A. W. Eckford, and R. A. Kennedy, "Convex optimization of distributed cooperative detection in multi-receiver molecular communication," *IEEE Trans. Mol., Biol. Multi-Scale Commun.*, vol. 3, no. 3, pp. 166–182, Sep. 2017.

[44] A. Shahbazi and A. Jamshidi, "Pre-coding technique for adaptive threshold detectors in diffusion-based molecular communications," in *Proc. 4th Int. Conf. Comput. Technol. Appl. (ICCTA)*, May 2018, pp. 59–63.

[45] A. Papoulis and S. U. Pillai, *Probability Random Variables and Stochastic Processes*. New York, NY, USA: McGraw-Hill, 2002.

[46] H. Birkan. (Jul. 2020). *Molecular Communication (Mucin) Simulator*. MATLAB Central File Exchange. [Online]. Available: https://www.mathworks.com/matlabcentral/fileexchange/46066-molecular-communication-mucin-simulator

[47] P. W. Alberts, A. Johnson, J. Lewis, M. Raff, and K. Roberts, *Molecular Biology of the Cell*, 5th ed. New York, NY, USA: Garland Science, 2007.

[48] M. Ş. Kuran, H. B. Yilmaz, T. Tugcu, and B. Özerman, "Energy model for communication via diffusion in nanonetworks," *Nano Commun. Netw.*, vol. 1, no. 2, pp. 86–95, Jun. 2010.

[49] N. Farsad, H. B. Yilmaz, C.-B. Chae, and A. Goldsmith, "Energy model for vesicle-based active transport molecular communication," in *Proc. IEEE Int. Conf. Commun. (ICC)*, May 2016, pp. 1–6.

TANIA ISLAM (Graduate Student Member, IEEE) received the B.Sc.Engg. degree in CSE from Patuakhali Science and Technology University (PSTU), Bangladesh, in 2012, the M.Sc. degree in CS from Jahangirnagar University (JU), Bangladesh, in 2014, and the M.Sc.Engg. degree in CSE from Khulna University (KU), Bangladesh, in 2018. She is currently pursuing the Ph.D. degree in information and communication engineering with Kyungpook National University, Daegu, South Korea. She was a Research Fellow with the ICT Division, Ministry of Posts, Telecommunications and Information Technology, Government of Peoples Republic, Bangladesh, in 2017. She is a Lecturer with the Computer Science and Engineering Department, University of Barishal (BU). Her research interests include molecular communication, wireless sensor networks, and medium access control protocol for wireless communication networks. She is a member of KICS. She was a recipient of the KNU International Graduate Scholarship (KINGS).

ETHUNGSHAN SHITIRI (Member, IEEE) received the B.E. degree in electronics and communication engineering from the Thanthai Periyar Government Institute of Technology, India, in 2010, the M.Tech. degree in communication systems from Christ University, India, in 2013, and the Ph.D. degree in information and communication engineering from Kyungpook National University, South Korea, in 2018. Since 2018, he has been a Postdoctoral Research Fellow with Kyungpook National University. His research interests include resource allocation, handshaking protocols, synchronization, and medium access techniques for wireless communication networks-namely cellular networks, M2M networks, underwater acoustic sensor networks, and molecular communication networks. He is a member of KICS. He was a recipient of the Kyungpook National University Honors Scholarship (KHS).

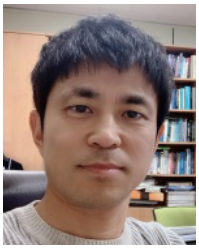

HO-SHIN CHO (Senior Member, IEEE) received the B.S., M.S., and Ph.D. degrees in electrical engineering from the Korea Advanced Institute of Science and Technology (KAIST), in 1992, 1994, and 1999, respectively.

From 1999 to 2000, he was a Senior Member of Research Staff with the Electronics and Telecommunications Research Institute (ETRI), where he was involved in developing a base station system for IMT-2000. From 2001 to 2002, he was a Faculty Member with the School of Electronics, Telecommunications, and Computer Engineering, Hankuk Aviation University. In 2003, he joined the School of Electronics Engineering, Kyungpook National University, as a Faculty Member, where he is currently a Professor. His current research interests include traffic engineering, radio resource management, and medium access control protocol for wireless communication networks, cellular networks, underwater communication, and molecular communication. He is a member of IEICE, IEEK, KICS, and ASK. He received the Rising Researcher Fellowship of NRF, in 1998.